

ELECTRONIC SUPPLEMENTARY INFORMATION

Low temperature pyrolytic route to amorphous quasi-hexagonal boron nitride from hydrogen rich $(\text{NH}_4)_3\text{Mg}(\text{BH}_4)_5$

Wojciech Wegner^{a,b}, Karol J. Fijalkowski^{b*}, Wojciech Grochala^b

a. College of Inter-Faculty Individual Studies in Mathematics and Natural Sciences, University of Warsaw, ul. Banacha 2c, 02-097 Warsaw, POLAND

b. Centre of New Technologies, University of Warsaw, ul. Banacha 2c, 02-097 Warsaw, POLAND

Contents:

01. Synthesis of $(\text{NH}_4)_3\text{Mg}(\text{BH}_4)_5$
02. Rietveld refinement of $(\text{NH}_4)_3\text{Mg}(\text{BH}_4)_5$
03. Attempts of purification of $(\text{NH}_4)_3\text{Mg}(\text{BH}_4)_5$ and complex of dibenzo-18-crown-6, NH_3BH_3 and DCM
04. Time resolved PXRD and FTIR measurements
05. Pyrolysis of $(\text{NH}_4)_3\text{Mg}(\text{BH}_4)_5$ and washing procedure
06. Extended TGA/DSC profiles
07. MAS NMR spectra
08. SEM and EDX analyses of $(\text{NH}_4)_3\text{Mg}(\text{BH}_4)_5$
09. Calculation of the yield of pyrolytic BN synthesis: elemental analysis and gravimetric study
10. Reaction route of pyrolytic BN synthesis

1. Synthesis of $(\text{NH}_4)_3\text{Mg}(\text{BH}_4)_5$

Chemicals were stored under argon atmosphere inside MBRAUN glovebox ($\text{O}_2 < 1 \text{ ppm}$, $\text{H}_2\text{O} < 1 \text{ ppm}$). All manipulations and reactions were carried out under argon atmosphere. Obtained products were stored in glovebox fridge at -43°C to ensure their stability. All the solvents, tools and containers used when processing the samples were pre-cooled to -43°C prior using. All the reagents were fine quality anhydrous chemicals purchased from Sigma Aldrich (LiBH_4 , NH_4Cl , MgCl_2 , DCM–dichloromethane) and Carl Roth (THF–tetrahydrofuran).

Synthesis of $(\text{NH}_4)_3\text{Mg}(\text{BH}_4)_5$ was attempted in a reaction between magnesium chloride, lithium borohydride and ammonium chloride in molar ratio of 1:5:3, leading to 1:5 molar ratio of $(\text{NH}_4)_3\text{Mg}(\text{BH}_4)_5$ and LiCl according to the following equation:



The reaction was performed in a mechanochemical procedure using in stainless steel milling bowl, pre-cooled with substrates inside in the glovebox fridge, using LMW–S vibrational mill from TESTCHEM (1400 rpm, *c.a.* 23.3 Hz). Milling was performed in 3 min periods, with standard overall time set to 18 min.

Two different synthesis temperature protocols were applied:

- the reaction mixture loaded to the mill was cooled with liquid nitrogen prior to milling (Eq.S1) and between the milling periods, temperature below 0°C was kept during the entire synthesis, 18 min, 30 min and 60 min milling time was tested
- milling was performed at room temperature and the product was placed at -43°C afterwards, 18 min milling was applied.

Reaction at molar ratio 1:4:2 was performed to check the alternative reaction pathway, but no $(\text{NH}_4)_2\text{Mg}(\text{BH}_4)_4$ was detected in the product. $(\text{NH}_4)_3\text{Mg}(\text{BH}_4)_5$ was the only product obtained, aside from LiCl by-product which, as shown below, acts merely as a ‘dead mass’ of the system.

2. Rietveld refinement of $(\text{NH}_4)_3\text{Mg}(\text{BH}_4)_5$

Rietveld refinement of a crystal structure of $(\text{NH}_4)_3\text{Mg}(\text{BH}_4)_5$ using powder diffraction data collected at -43°C . LiCl can be seen as a dominant phase being a by-product of the synthesis of $(\text{NH}_4)_3\text{Mg}(\text{BH}_4)_5$. 5% impurity fraction of NH_4BH_4 was observed in numerous samples milled at low temperature for 18–60 minutes. No Cl substitution for BH_4 anion was observed; the fits assuming full occupancy of ammonium sites by NH_4^+ cations led to the best fit.

Presence of NH_4BH_4 in the sample of $(\text{NH}_4)_3\text{Mg}(\text{BH}_4)_5$ can be explained either as a by-product of some competing reaction occurring during the milling, or as a product of thermal decomposition of $(\text{NH}_4)_3\text{Mg}(\text{BH}_4)_5$. If the first hypothesis was true, we would expect varying amounts of NH_4BH_4 in the sample depending in the milling time, which was not observed. If the second scenario was true, we would expect also formation of $\text{Mg}(\text{BH}_4)_2$ or some relating compound, however, formation of amorphous $\text{Mg}(\text{BH}_4)_2$ in other processes has been already reported in the literature [5].

Molar ratio of $(\text{NH}_4)_3\text{Mg}(\text{BH}_4)_5$ to LiCl according to proposed synthesis reaction equals 1:5, but as a result of Rietveld refinement we get the value of 1:10. This discrepancy originates from several factors related to crystallinity and stability of $(\text{NH}_4)_3\text{Mg}(\text{BH}_4)_5$, which were far beyond our control. In general, mechanochemically obtained materials are of low crystallinity, which can be enhanced by high temperature annealing; however, thermal annealing is not possible in the case of $(\text{NH}_4)_3\text{Mg}(\text{BH}_4)_5$ as this compound is unstable already at room temperature. Very low thermal stability of $(\text{NH}_4)_3\text{Mg}(\text{BH}_4)_5$ was also manifested by partial decomposition of the material during transportation to diffractometer, as evidenced by presence of NH_4BH_4 reflections in PXRD pattern. The sample might also undergo partial amorphisation prior to PXRD measurements. Due to low stability of $(\text{NH}_4)_3\text{Mg}(\text{BH}_4)_5$ better experimental data were out of reach.

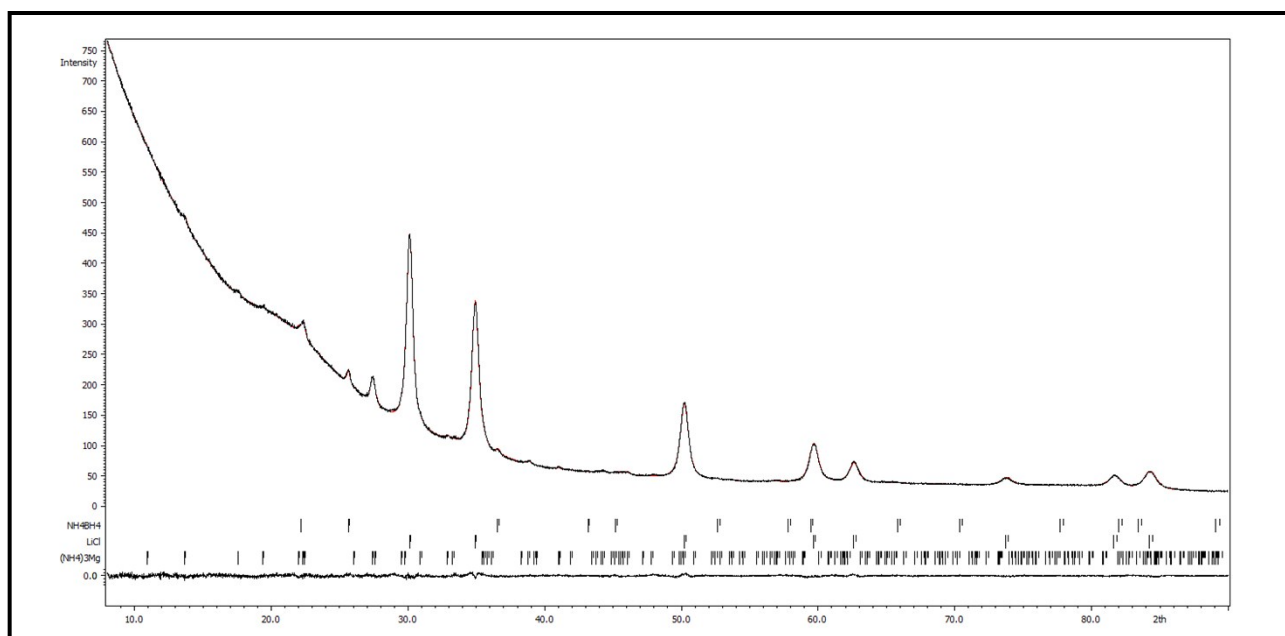


Figure S2.1. Rietveld refinement of crystal structure of $(\text{NH}_4)_3\text{Mg}(\text{BH}_4)_5$. $R_{wp} = 0.97$, $\text{GOF} = 0.12$.

3. Attempts of purification of $(\text{NH}_4)_3\text{Mg}(\text{BH}_4)_5$ and complex of dibenzo-18-crown-6, NH_3BH_3 and DCM

Due to the presence of large quantities of LiCl in the samples of $(\text{NH}_4)_3\text{Mg}(\text{BH}_4)_5$ we attempted to separate these components by dissolving $(\text{NH}_4)_3\text{Mg}(\text{BH}_4)_5$ in organic solvent and its further recrystallisation. Since $(\text{NH}_4)_3\text{Mg}(\text{BH}_4)_5$ is sensitive to moisture we could not rinse LiCl with water.

Solubility of $(\text{NH}_4)_3\text{Mg}(\text{BH}_4)_5$ was checked using solvents (THF, DCM) precooled to -43°C . After adding THF at -43°C , sample immediately started releasing gas violently and powder was still present at the bottom of flask. After the separation of liquid and powder, both of them were left at -43°C to evaporate THF. Even after more than 4 months both fractions had still gel consistency.

After adding DCM to $(\text{NH}_4)_3\text{Mg}(\text{BH}_4)_5$ at -43°C there no gas was released. After removing the solvent at -43°C FTIR spectrum was collected, which didn't change at RT in time and was similar to the spectrum obtained after the decomposition of $(\text{NH}_4)_3\text{Mg}(\text{BH}_4)_5$ at RT. As $(\text{NH}_4)_3\text{Mg}(\text{BH}_4)_5$ slowly decomposed in DCM, after dissolving it in DCM we immediately add it to dibenzo-18-crown-6 dissolved also in DCM at -43°C . After removing the solvent, single crystal was obtained and resulting phase was identified as dibenzo-18-crown-6 with molecule of NH_3BH_3 and DCM, which is isostructural to the same compound with NH_3BF_3 [1] molecule instead of AB. At collected PXRD pattern, this was identified as the only crystal phase present in the sample, suggesting decomposition of the sample in DCM.

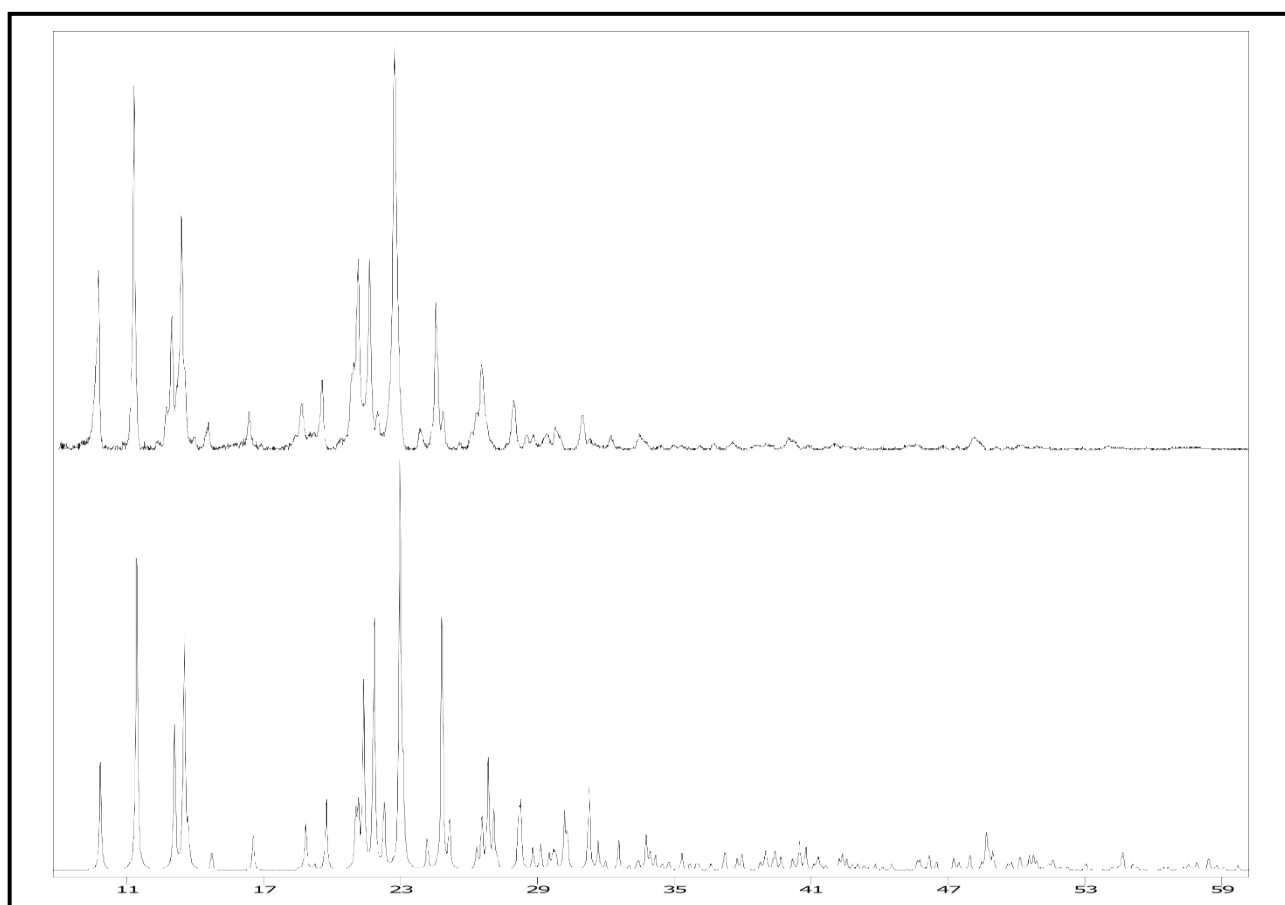


Figure S3.1. Comparison of a diffractogram of a complex of dibenzo-18-crown-6 with NH_3BH_3 and DCM (bottom) with a diffractogram calculated from a preliminary monocrystalline structural model

4. Time resolved PXR and FTIR measurements

Time resolved FTIR and XRD measurements were performed for $(\text{NH}_4)_3\text{Mg}(\text{BH}_4)_5$ cooled to -43°C . The sample was allowed to warm up to room temperature throughout the whole experiment. Comparison of the sequential experimental data reveal decomposition of $(\text{NH}_4)_3\text{Mg}(\text{BH}_4)_5$ upon heating from -43°C to RT in vacuum, in a KBr pellet.

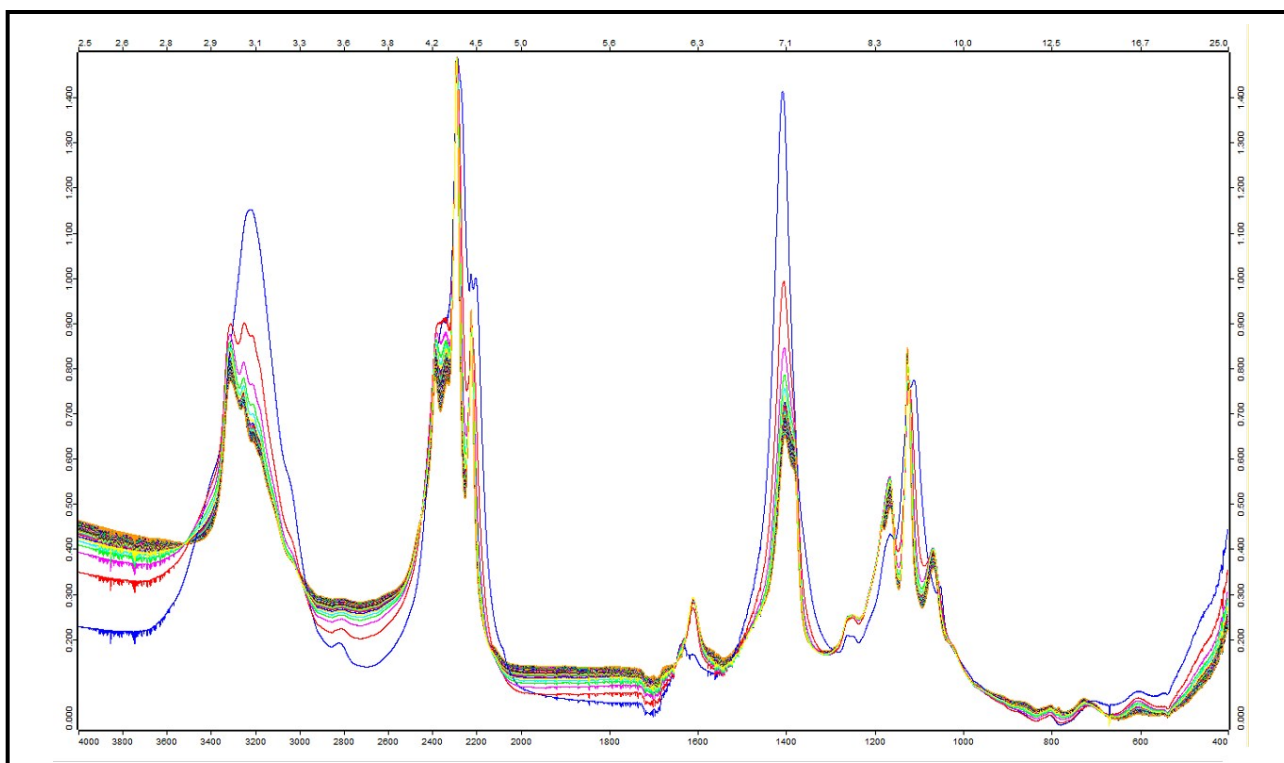


Figure S5.1. Series of FTIR spectra of freshly prepared $(\text{NH}_4)_3\text{Mg}(\text{BH}_4)_5$ taken at a room temperature with an interval of 5–10 min.

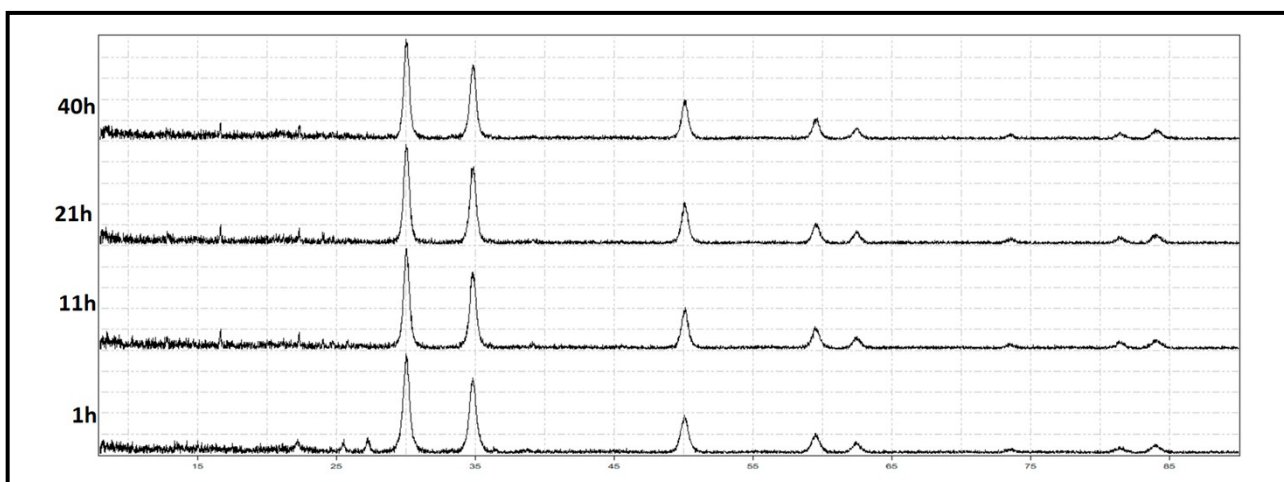


Figure S5.2. Series of PXR pattern of freshly prepared $(\text{NH}_4)_3\text{Mg}(\text{BH}_4)_5$ taken at room temperature with an interval of 1h (selected patterns showed after 1h, 11h, 21h and 40h).

5. Pyrolysis of $(\text{NH}_4)_3\text{Mg}(\text{BH}_4)_5$ and washing procedure

Decrease of heating rate from $5^\circ\text{C}/\text{min}$ to $1^\circ\text{C}/\text{min}$ led to change of maximum rate of the first decomposition process from 46°C to 32°C and decrease of purity of evolved hydrogen, while changing heating rate to 50°C changed maximum to 80°C and also decreased the purity of evolved hydrogen.

Sample heated to 500°C was rinsed with water and FTIR spectra and PXRD pattern were obtained, after removing remaining water by heating it for 30 min at 80°C and then for 60 min at 90°C . No crystal product was detected at PXRD pattern, LiCl and additional phases (*i.a.* MgO) were washed out. Simultaneously, amorphous BN remained in the sample, what can be seen at FTIR spectrum with characteristic bands around 1400 cm^{-1} and 800 cm^{-1} , which resemble more a highly ordered h-BN rather than pyrolytic amorphous BN.

After collecting MAS NMR spectra for sample heated to 650°C that sample was further rinsed with water six times, by slowly decantation of the solid and removing the liquid using the syringe. After that the precipitate was dried in vacuum and SEM/EDX datasets were collected. Their description is given in the main manuscript.

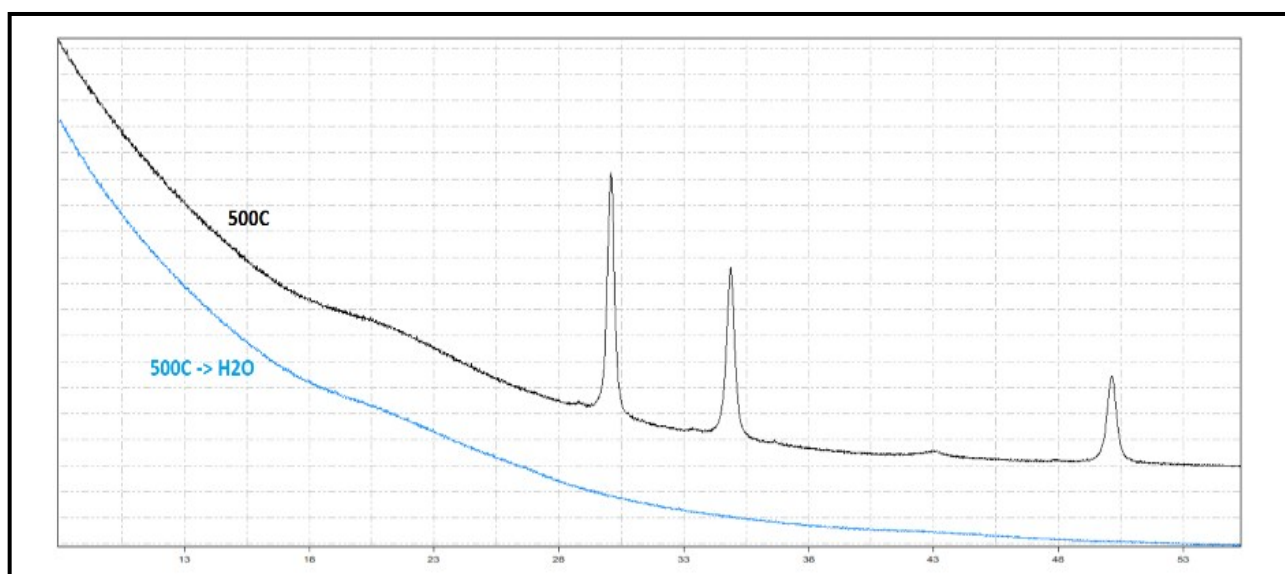


Figure S3.1. PXRD patterns of $(\text{NH}_4)_3\text{Mg}(\text{BH}_4)_5$ after exposing to 500°C and after rinsing sample preheated to 500°C with water.

6. Extended TGA/DSC profiles

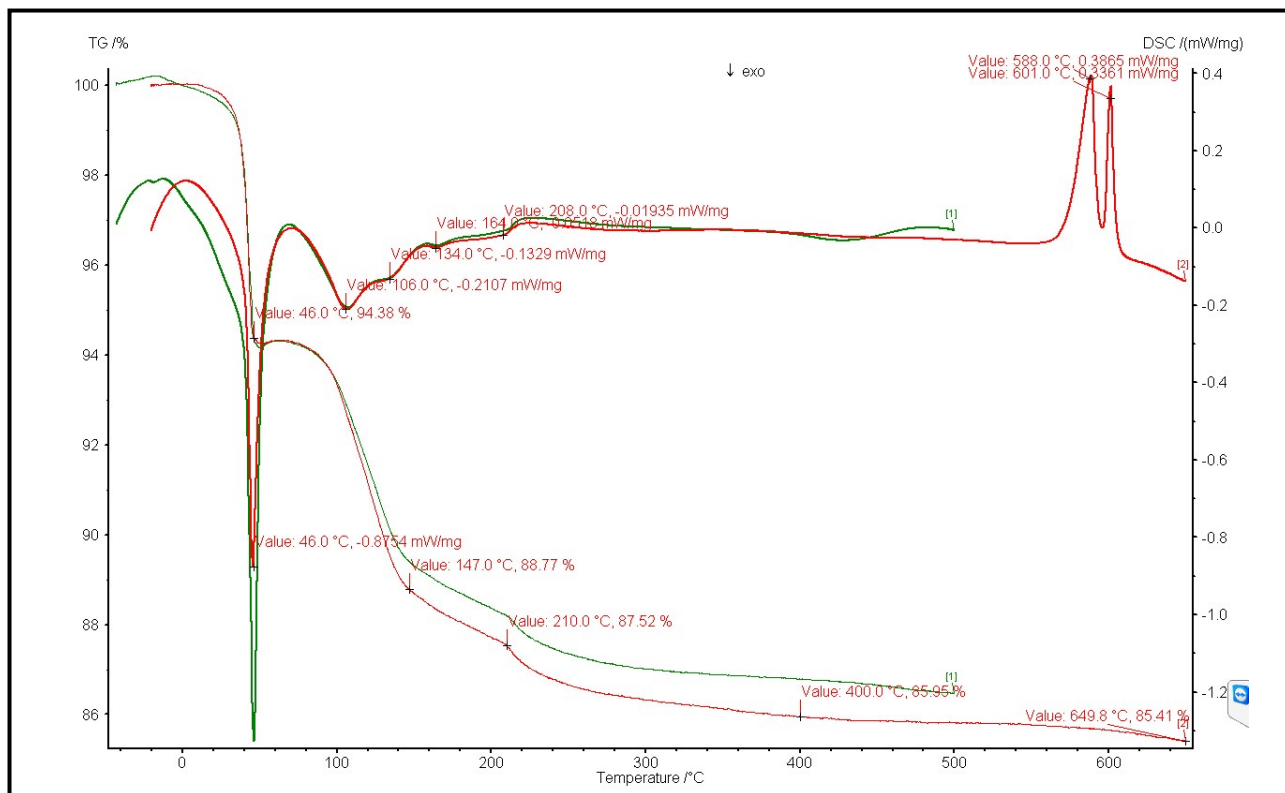


Figure S6.1. TGA/DSC profiles of $(\text{NH}_4)_3\text{Mg}(\text{BH}_4)_5$ in the temperature range of $(-20^{\circ}\text{C})-(+650^{\circ}\text{C})$ and $(-43^{\circ}\text{C})-(+500^{\circ}\text{C})$ at 5K/min heating rate. Peak position indicated for each exothermic process.

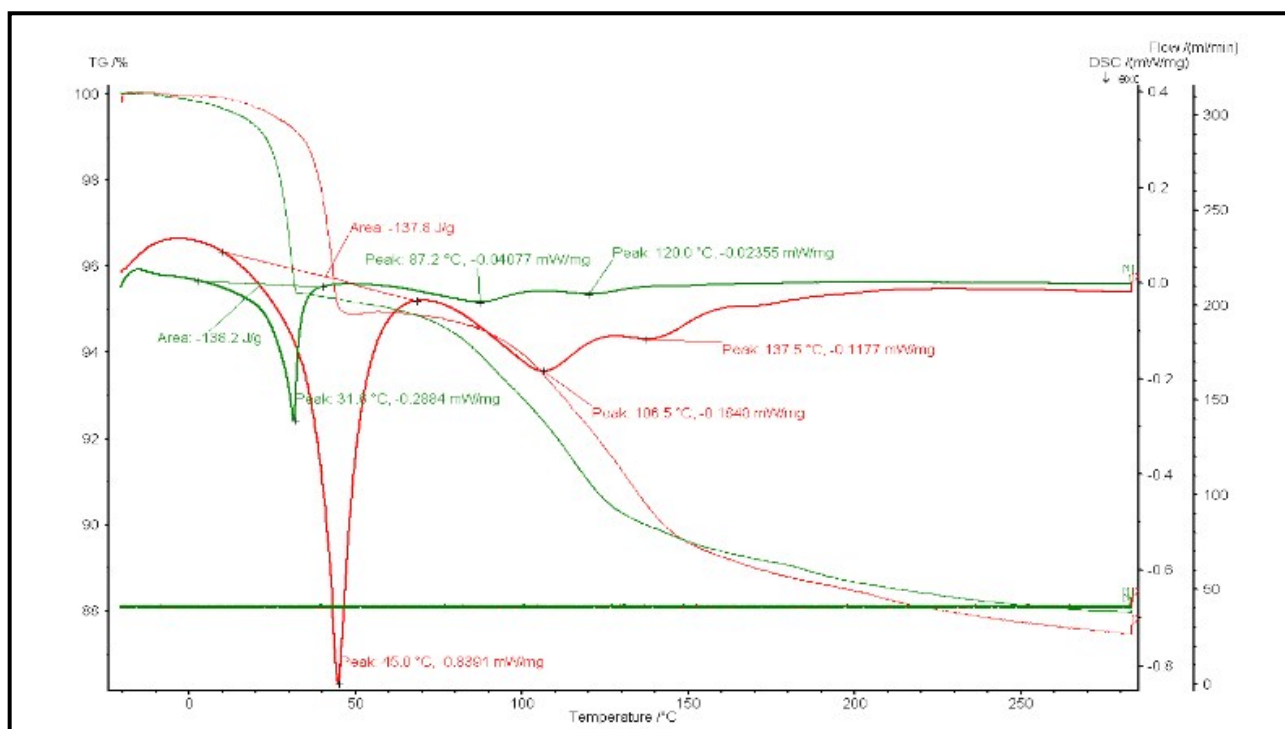


Figure S6.2. TGA/DSC profiles of $(\text{NH}_4)_3\text{Mg}(\text{BH}_4)_5$ in the temperature range of $(-20^{\circ}\text{C})-(+270^{\circ}\text{C})$ at 1K/min (green) and 5K/min (red) heating rate. Peak position indicated for each exothermic process.

7. NMR spectra

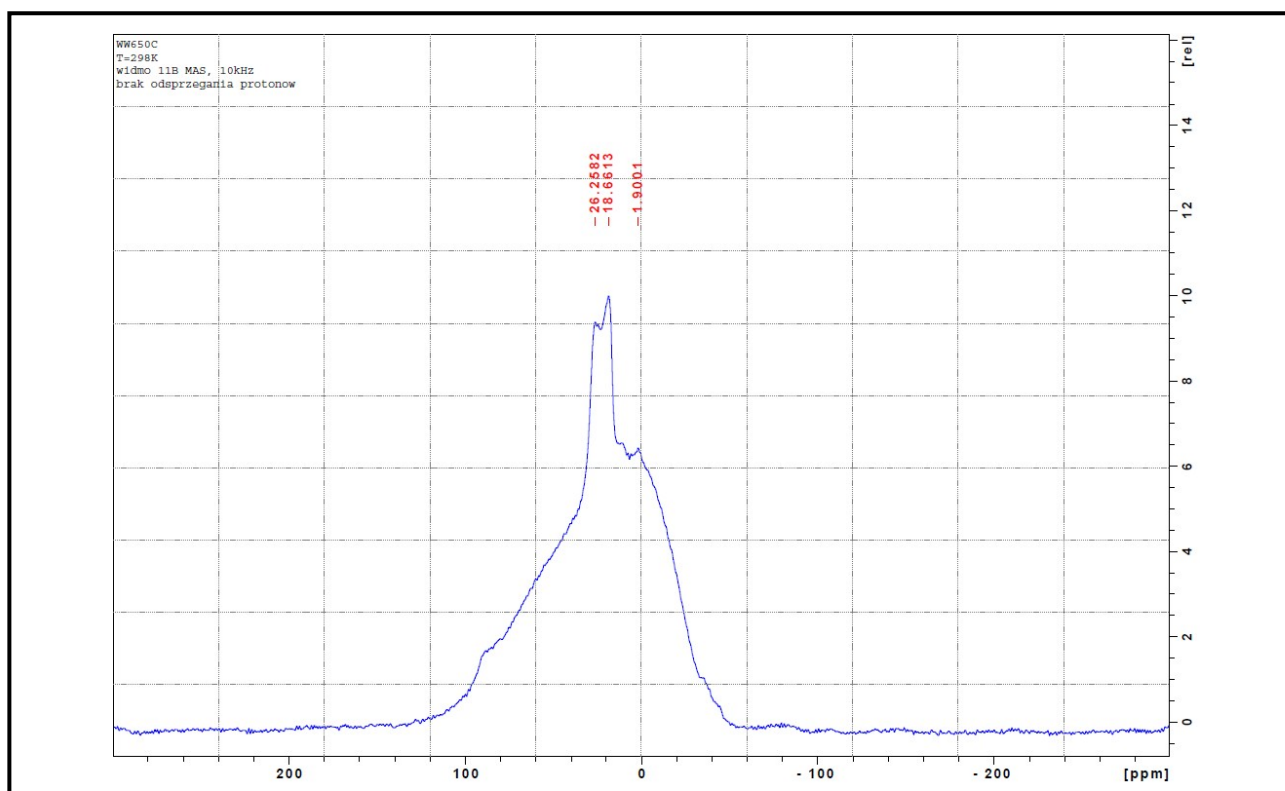


Figure S7.1. ^{11}B MAS NMR spectra of $(\text{NH}_4)_3\text{Mg}(\text{BH}_4)_5$ heated to 650°C , without proton decoupling.

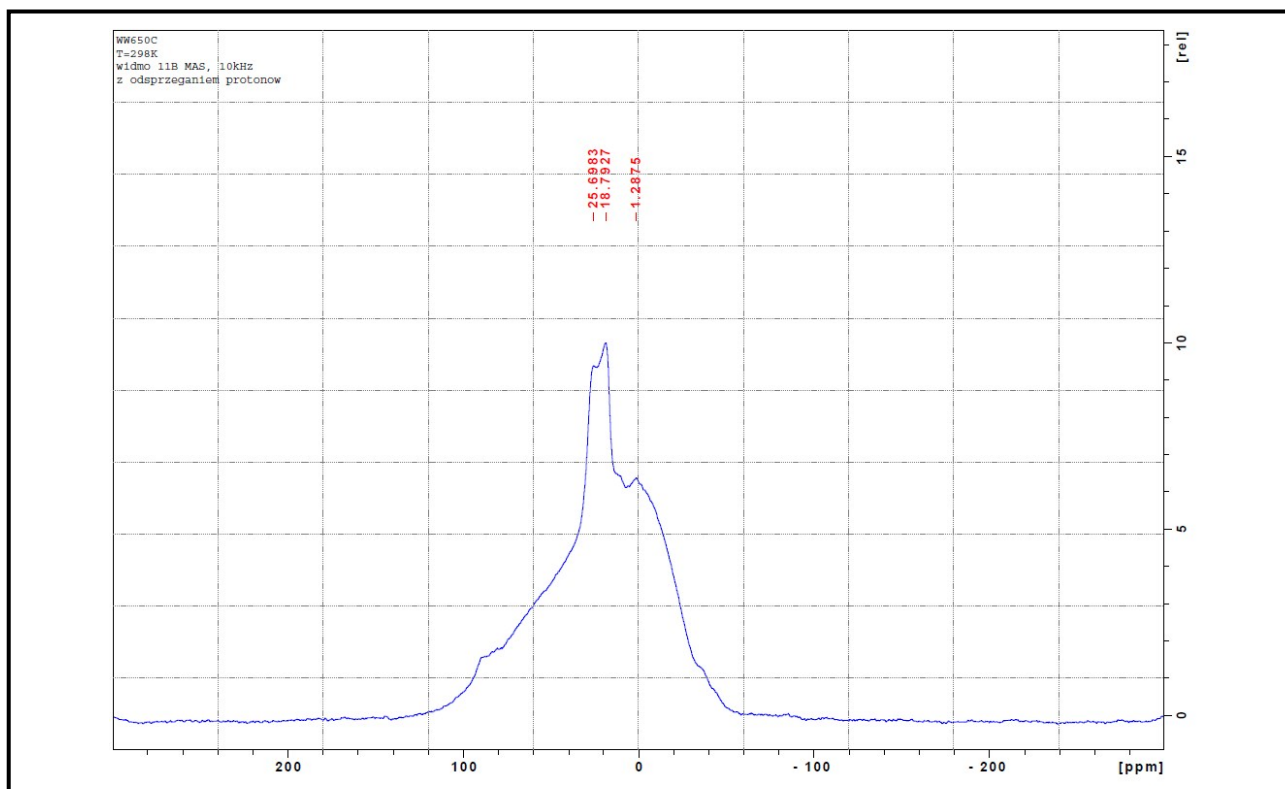


Figure S7.2. ^{11}B MAS NMR spectra of $(\text{NH}_4)_3\text{Mg}(\text{BH}_4)_5$ heated to 650°C , with proton decoupling.

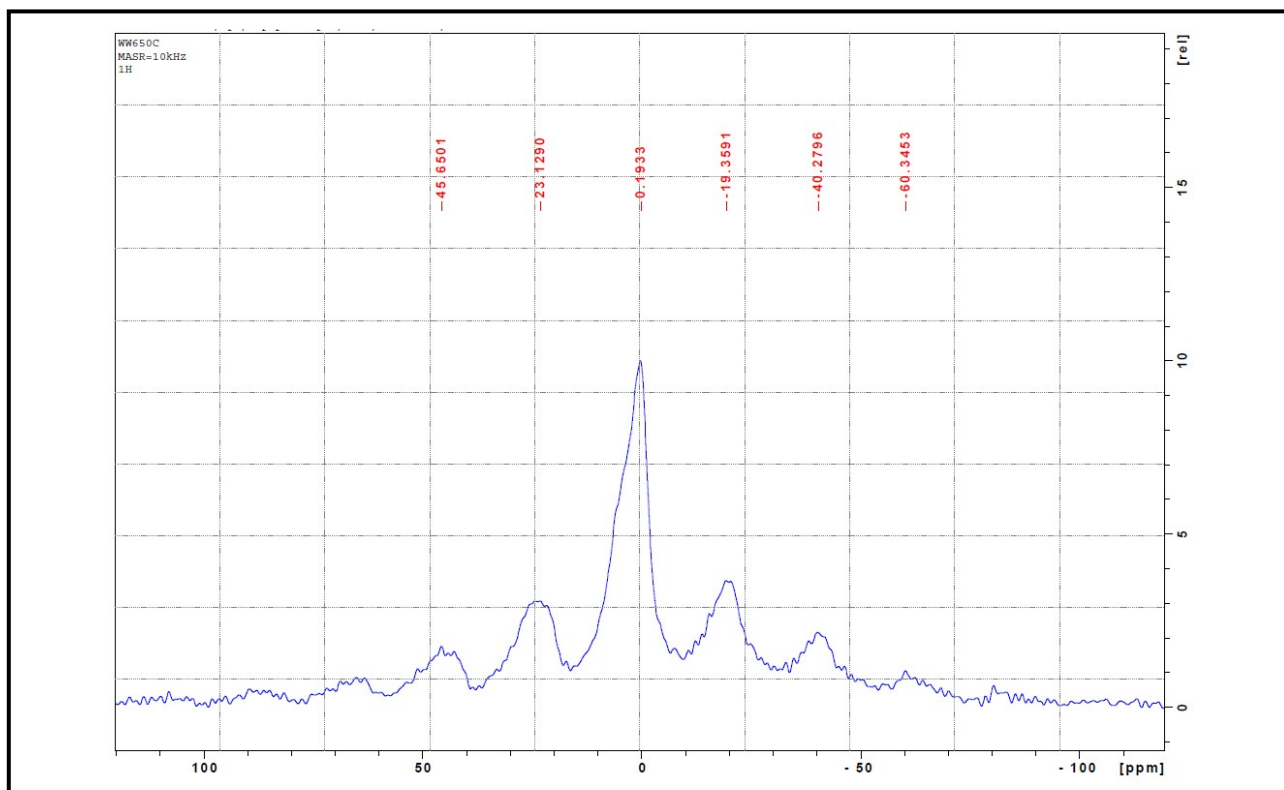


Figure S7.3. ^1H MAS NMR spectra of $(\text{NH}_4)_3\text{Mg}(\text{BH}_4)_5$ heated to 650°C .

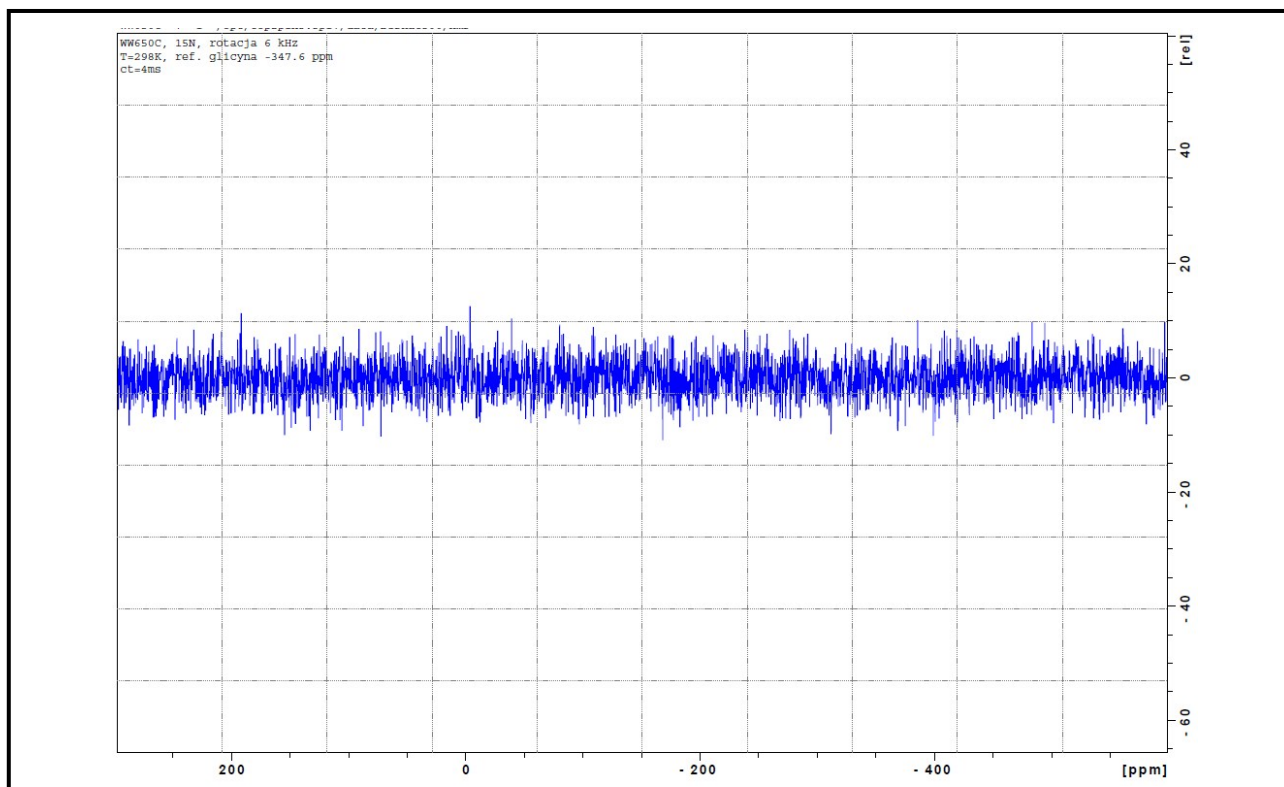


Figure S7.4. ^{15}N MAS NMR spectrum of $(\text{NH}_4)_3\text{Mg}(\text{BH}_4)_5$ heated to 650°C , collected overnight.

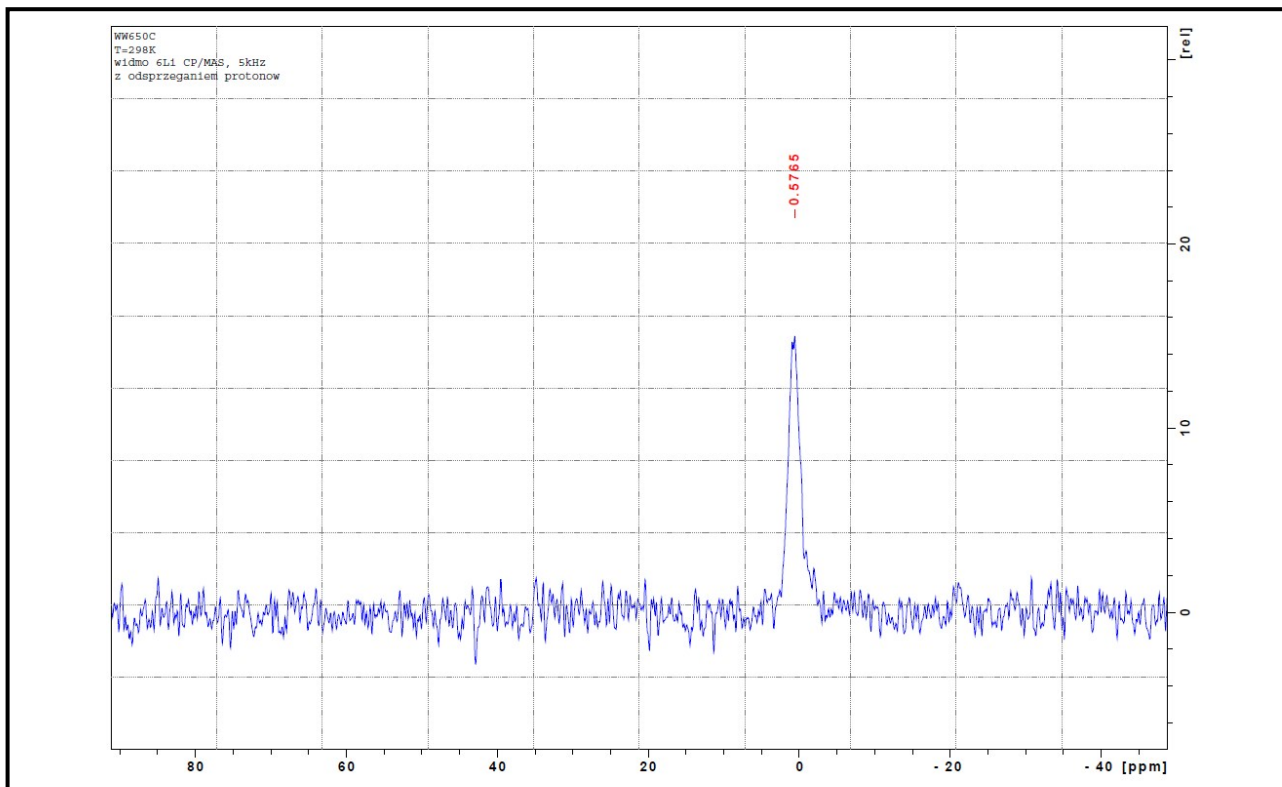


Figure S7.5. ^6Li MAS NMR spectra of $(\text{NH}_4)_3\text{Mg}(\text{BH}_4)_5$ heated to 650°C .

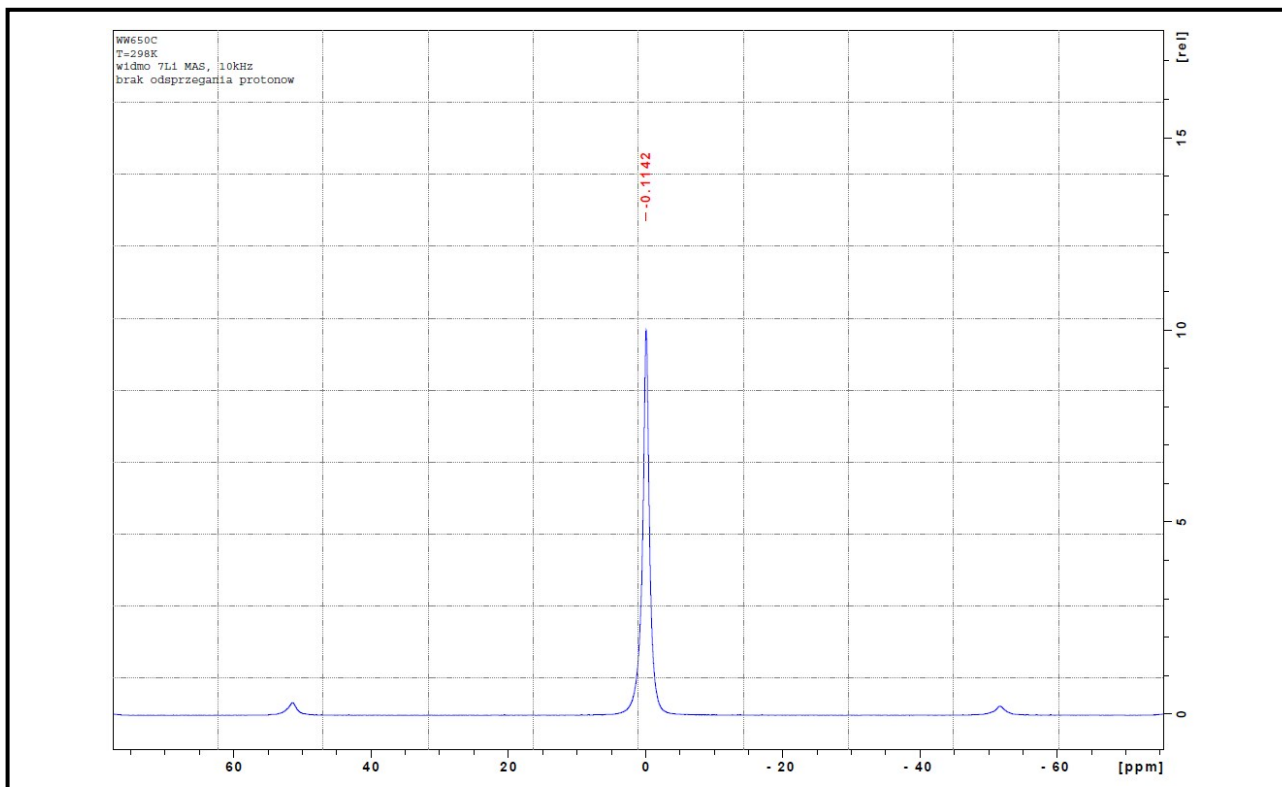


Figure S7.6. ^7Li MAS NMR spectra of $(\text{NH}_4)_3\text{Mg}(\text{BH}_4)_5$ heated to 650°C .

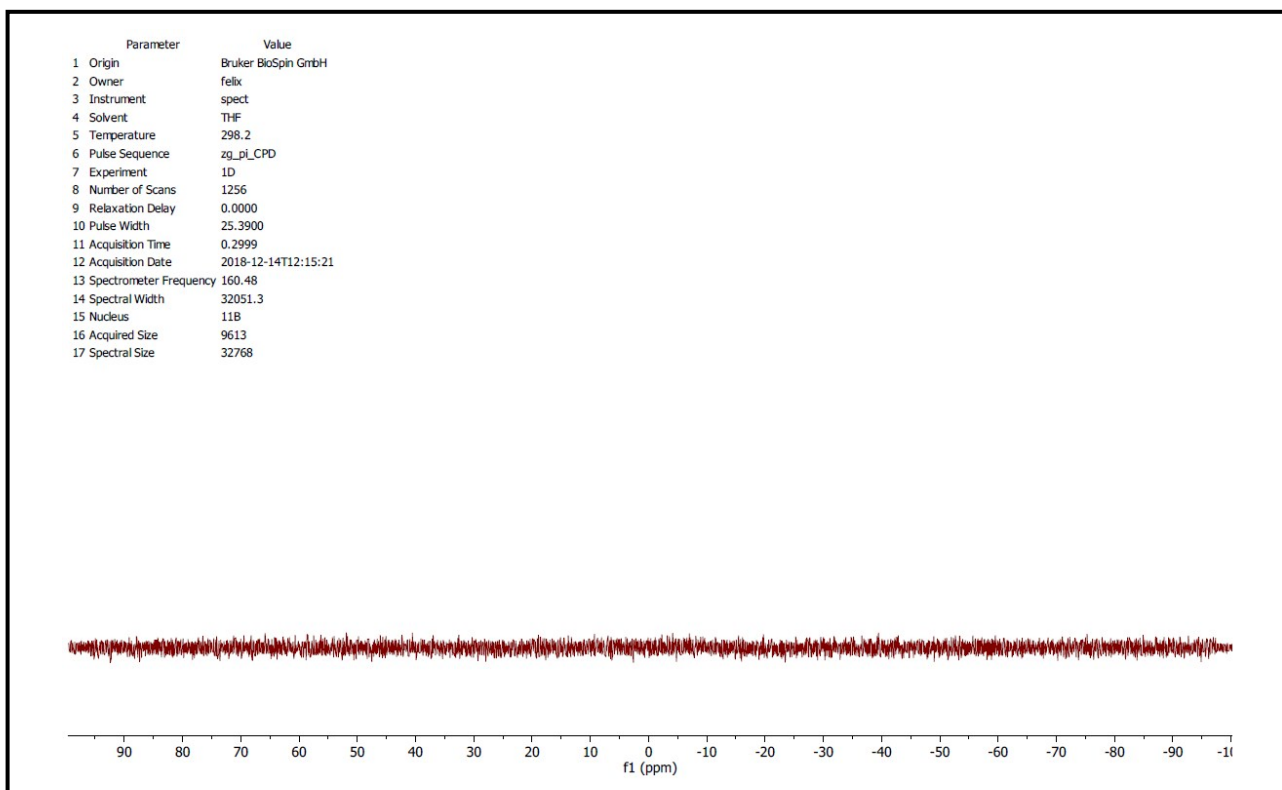


Figure S7.7. ^{11}B NMR spectra of $(\text{NH}_4)_3\text{Mg}(\text{BH}_4)_5$ heated to 500°C and the residue dissolved in THF-d_8 .

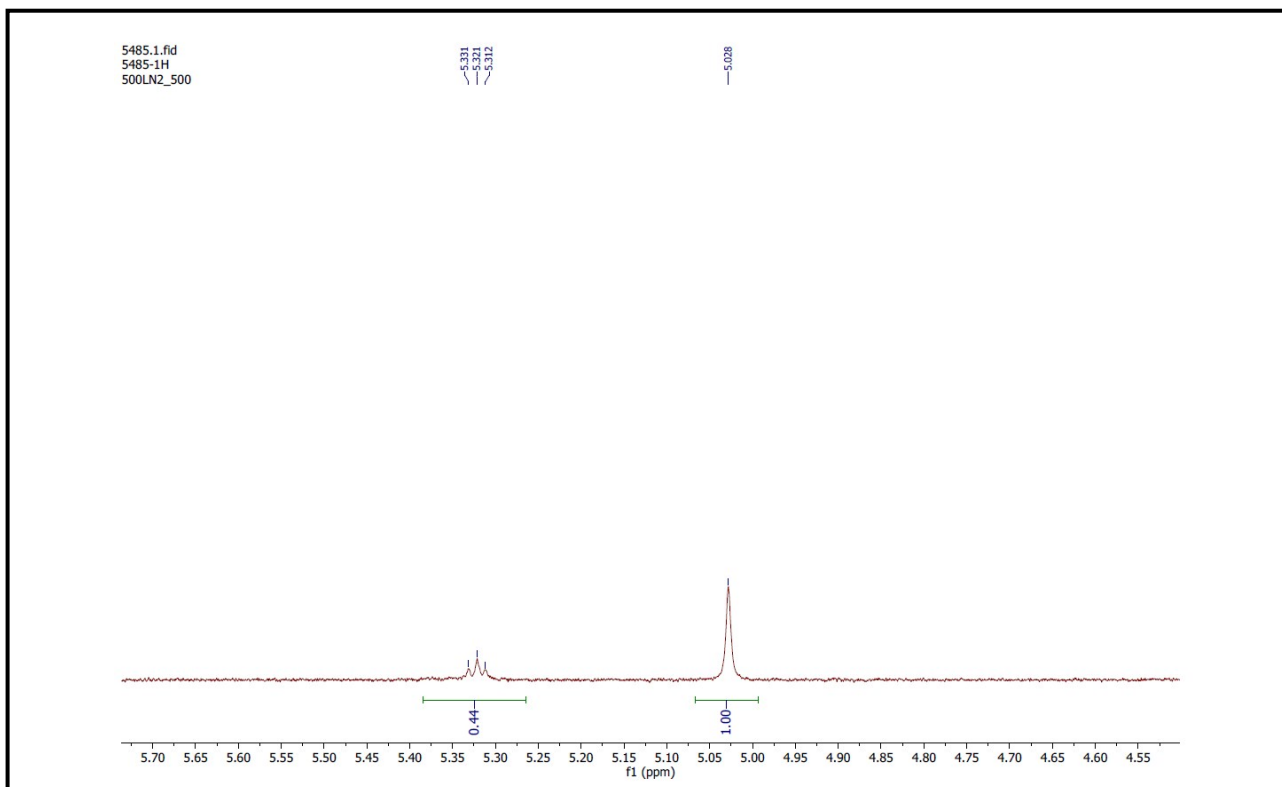


Figure S7.8. ^1H NMR spectra of $(\text{NH}_4)_3\text{Mg}(\text{BH}_4)_5$ heated to 500°C and the residue dissolved in THF-d_8 .

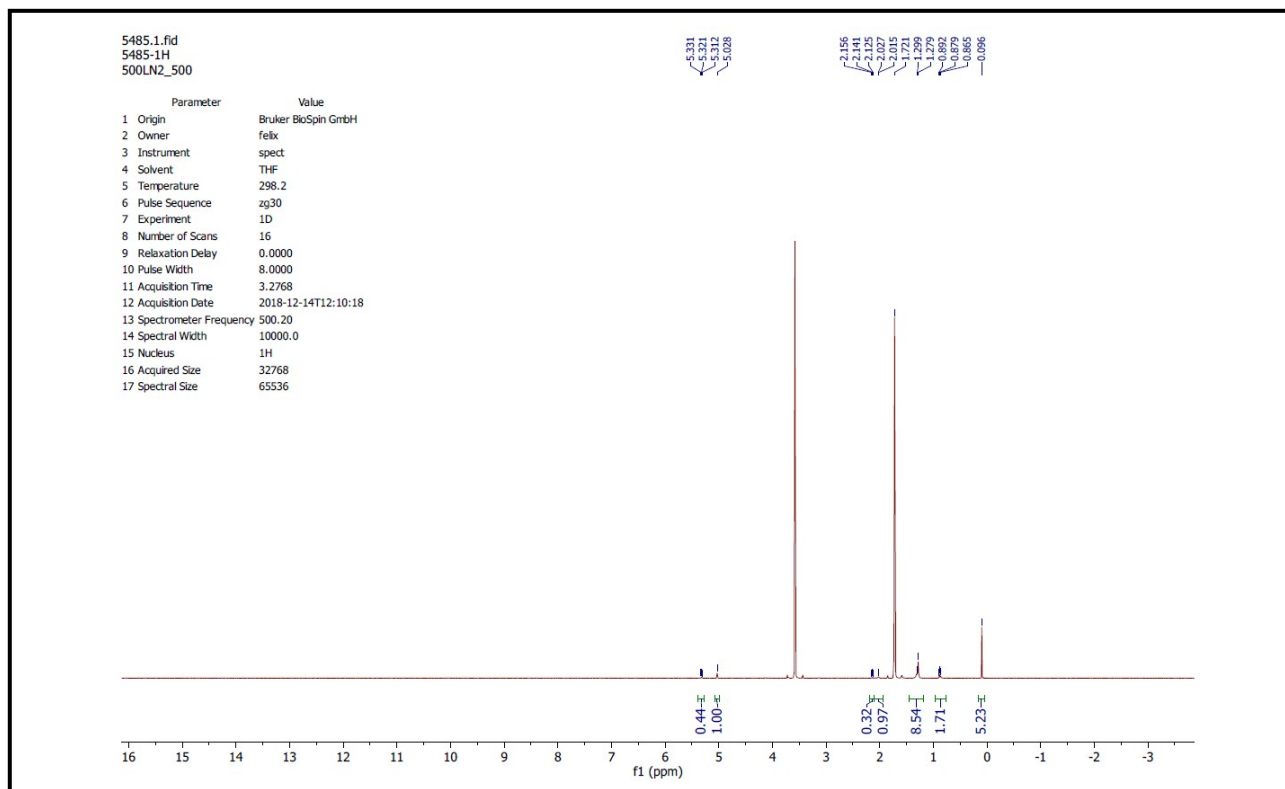


Figure S7.9. ^1H NMR spectra of $(\text{NH}_4)_3\text{Mg}(\text{BH}_4)_5$ heated to 500°C and the residue dissolved in THF-d_8 .

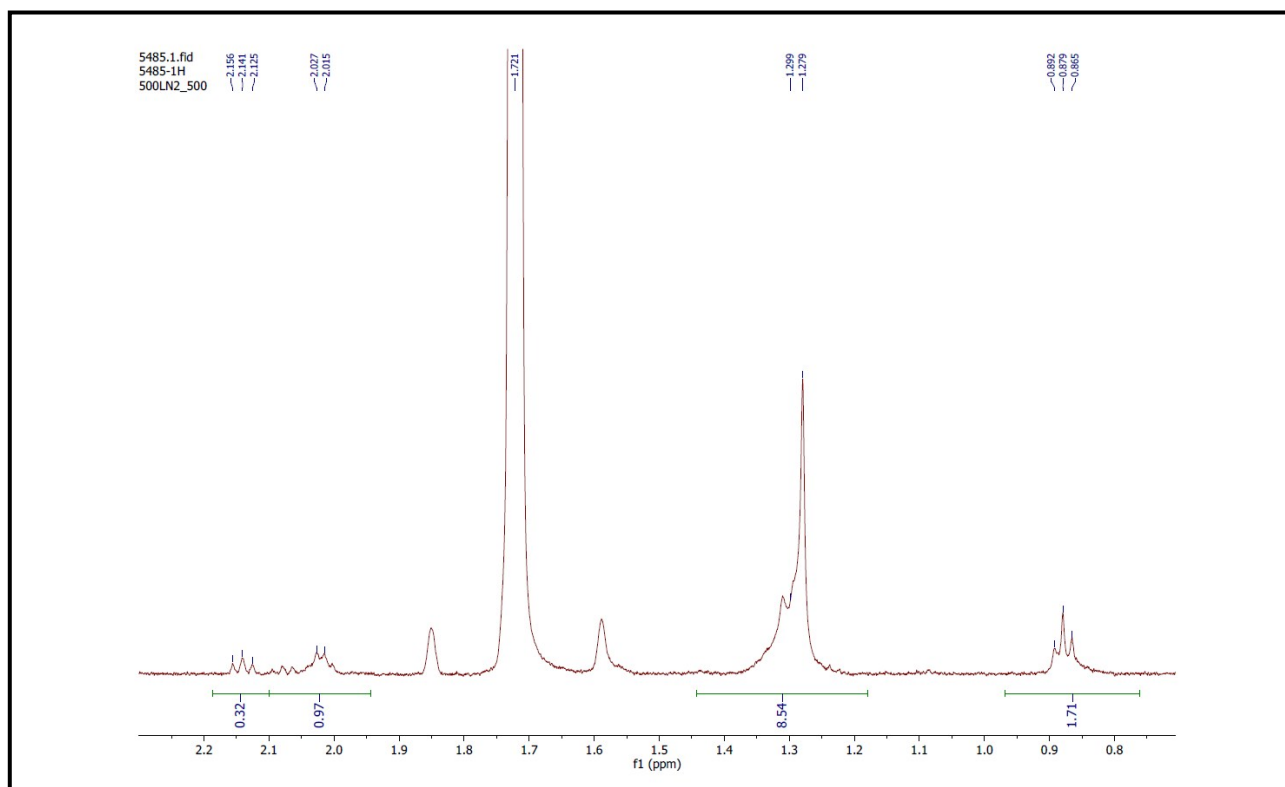


Figure S7.10. ^1H NMR spectra of $(\text{NH}_4)_3\text{Mg}(\text{BH}_4)_5$ heated to 500°C and the residue dissolved in THF-d_8 .

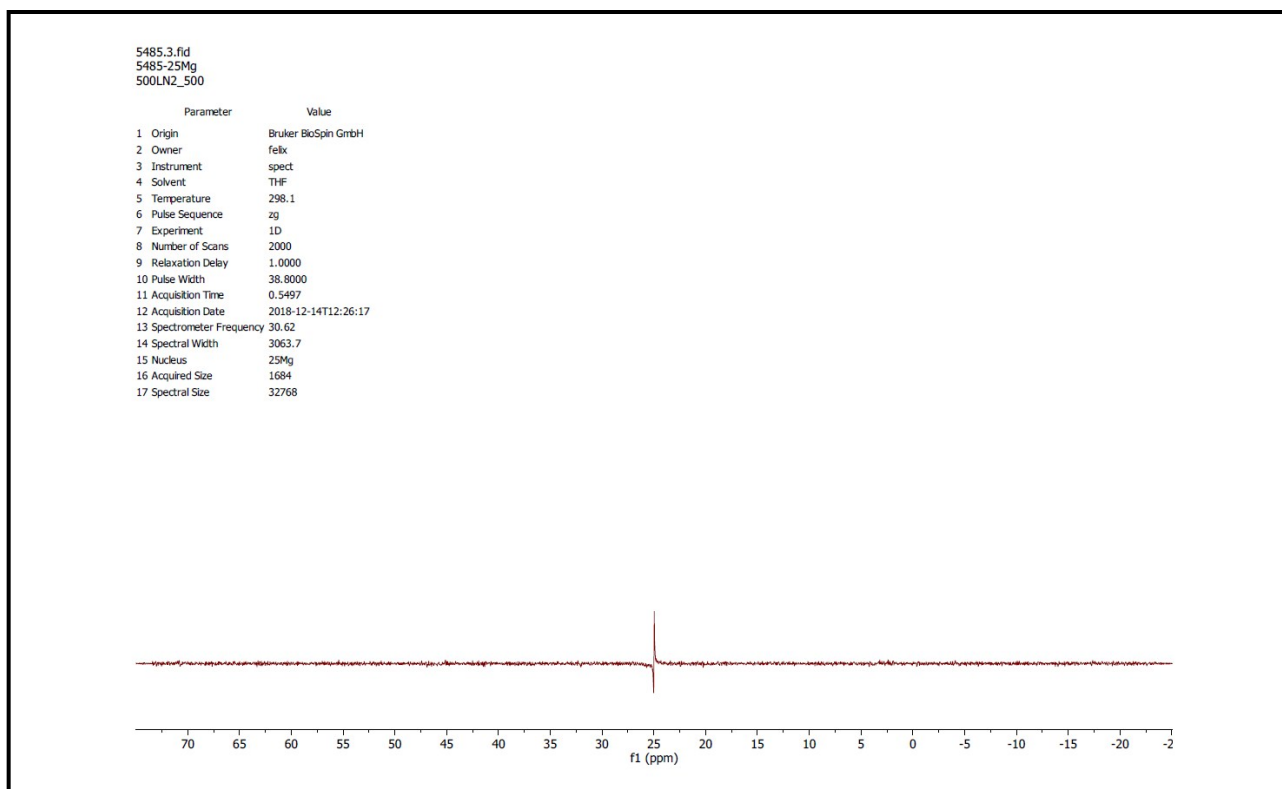


Figure S7.11. ^{25}Mg NMR spectra of $(\text{NH}_4)_3\text{Mg}(\text{BH}_4)_5$ heated to 500°C and the residue dissolved in THF-d_8 .

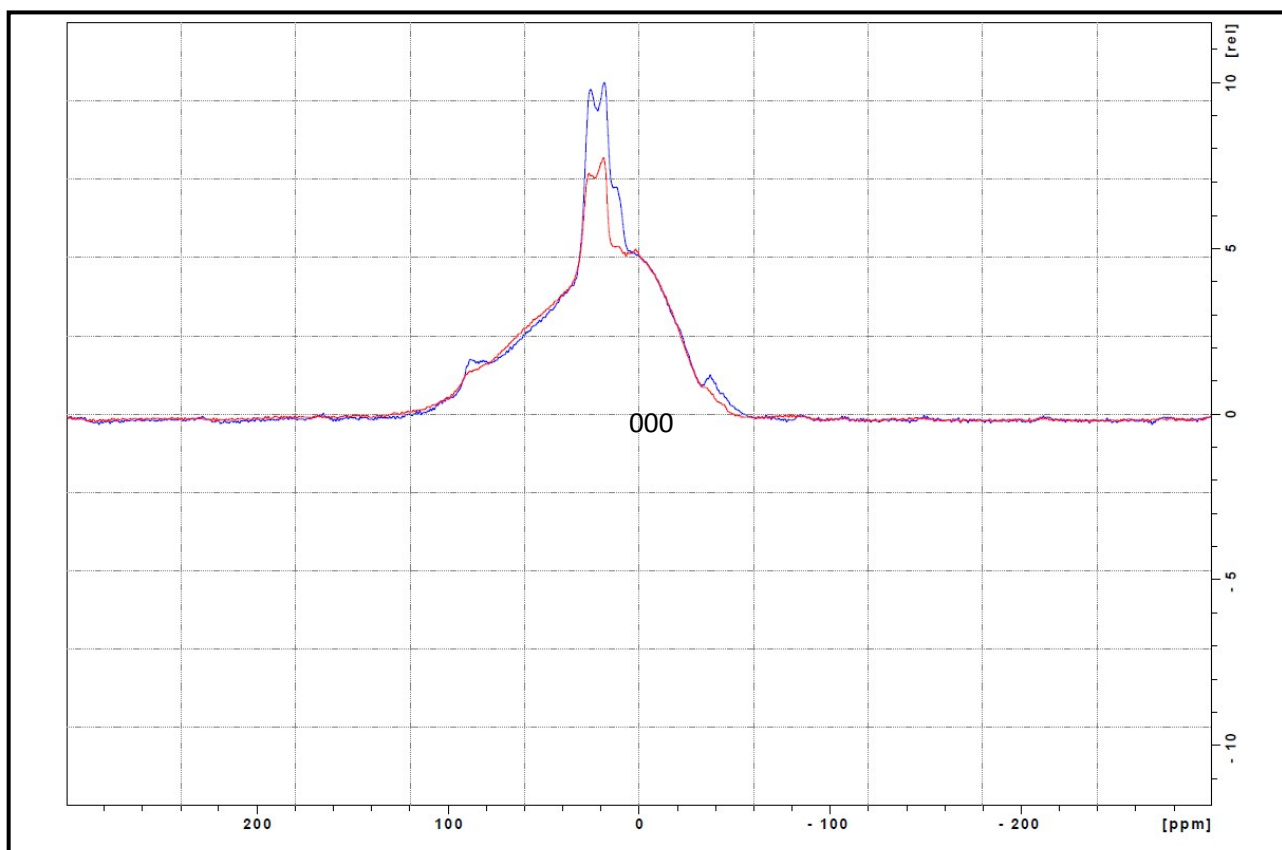


Figure S7.12. ^{11}B MAS NMR spectra of $(\text{NH}_4)_3\text{Mg}(\text{BH}_4)_5$ heated to 650°C and of reference h-BN. No background subtraction.

8. SEM and EDX analyses of $(\text{NH}_4)_3\text{Mg}(\text{BH}_4)_5$

Atomic ratio of nitrogen and boron in the samples of $(\text{NH}_4)_3\text{Mg}(\text{BH}_4)_5$ heated to 650°C and 5 times rinsed with fresh portion of distilled water, measured with EDX method, is close to **1:1**, suggesting the formation of boron nitride.

Table S8.1. EDX analysis of a selected spot of $(\text{NH}_4)_3\text{Mg}(\text{BH}_4)_5$ sample heated to 650°C and 5 times rinsed with distilled water. Carbon tape used as a surface. The sample was loaded at normal atmosphere.

$$\text{B} / \text{N} = 21.56 / 22.74 = \mathbf{1 : 0.95}$$

| Element | Series | unn. C [wt.%] | norm. C [at.%] | Atom. C | Error (1 Sigma) [wt.%] |
|-----------|----------|------------------|-------------------|---------|---------------------------|
| Magnesium | K-series | 2.29 | 2.29 | 1.22 | 0.15 |
| Oxygen | K-series | 19.33 | 19.33 | 15.70 | 2.39 |
| Nitrogen | K-series | 24.51 | 24.51 | 22.74 | 3.15 |
| Carbon | K-series | 35.78 | 35.78 | 38.71 | 4.20 |
| Silicon | K-series | 0.11 | 0.11 | 0.05 | 0.03 |
| Boron | K-series | 17.93 | 17.93 | 21.56 | 2.67 |
| Chlorine | K-series | 0.05 | 0.05 | 0.02 | 0.03 |
| Total: | | 100.00 | 100.00 | 100.00 | |

Table S8.2. EDX analysis of a selected spot of $(\text{NH}_4)_3\text{Mg}(\text{BH}_4)_5$ sample heated to 650°C and rinsed 5 times with water. Carbon tape used as a surface. The sample was loaded at normal atmosphere.

$$\text{B} / \text{N} = 27.15 / 25.15 = \mathbf{1 : 1.08}$$

| Element | Series | unn. C [wt.%] | norm. C [at.%] | Atom. C | Error (1 Sigma) [wt.%] |
|-----------|----------|------------------|-------------------|---------|---------------------------|
| Magnesium | K-series | 1.82 | 1.82 | 0.98 | 0.12 |
| Oxygen | K-series | 21.78 | 21.78 | 17.73 | 2.78 |
| Nitrogen | K-series | 27.04 | 27.04 | 25.15 | 3.58 |
| Carbon | K-series | 26.65 | 26.65 | 28.91 | 3.41 |
| Silicon | K-series | 0.14 | 0.14 | 0.07 | 0.03 |
| Boron | K-series | 22.53 | 22.53 | 27.15 | 3.49 |
| Chlorine | K-series | 0.04 | 0.04 | 0.02 | 0.03 |
| Total: | | 100.00 | 100.00 | 100.00 | |

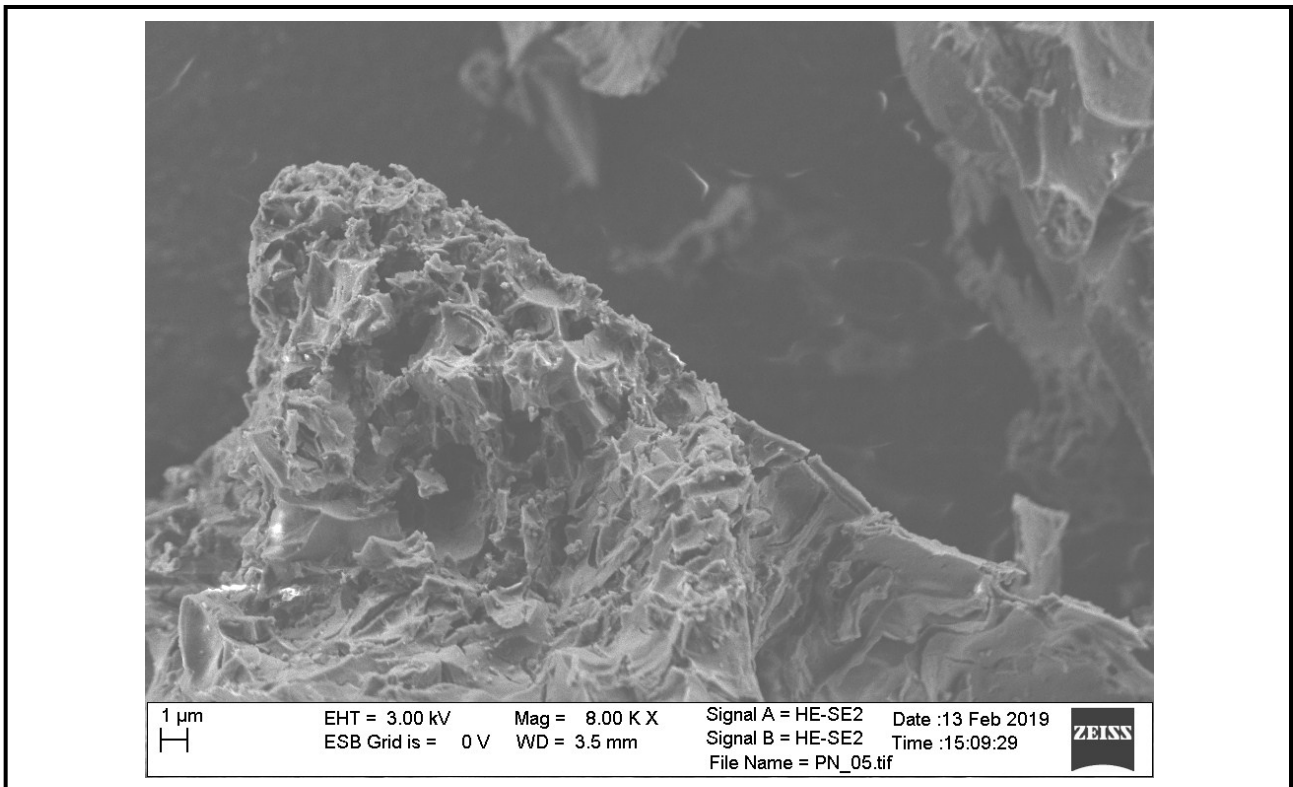


Figure S8.3. SEM image of $(\text{NH}_4)_3\text{Mg}(\text{BH}_4)_5$ sample heated to 650°C and rinsed 5 times with water. Magnification 8.00 KX

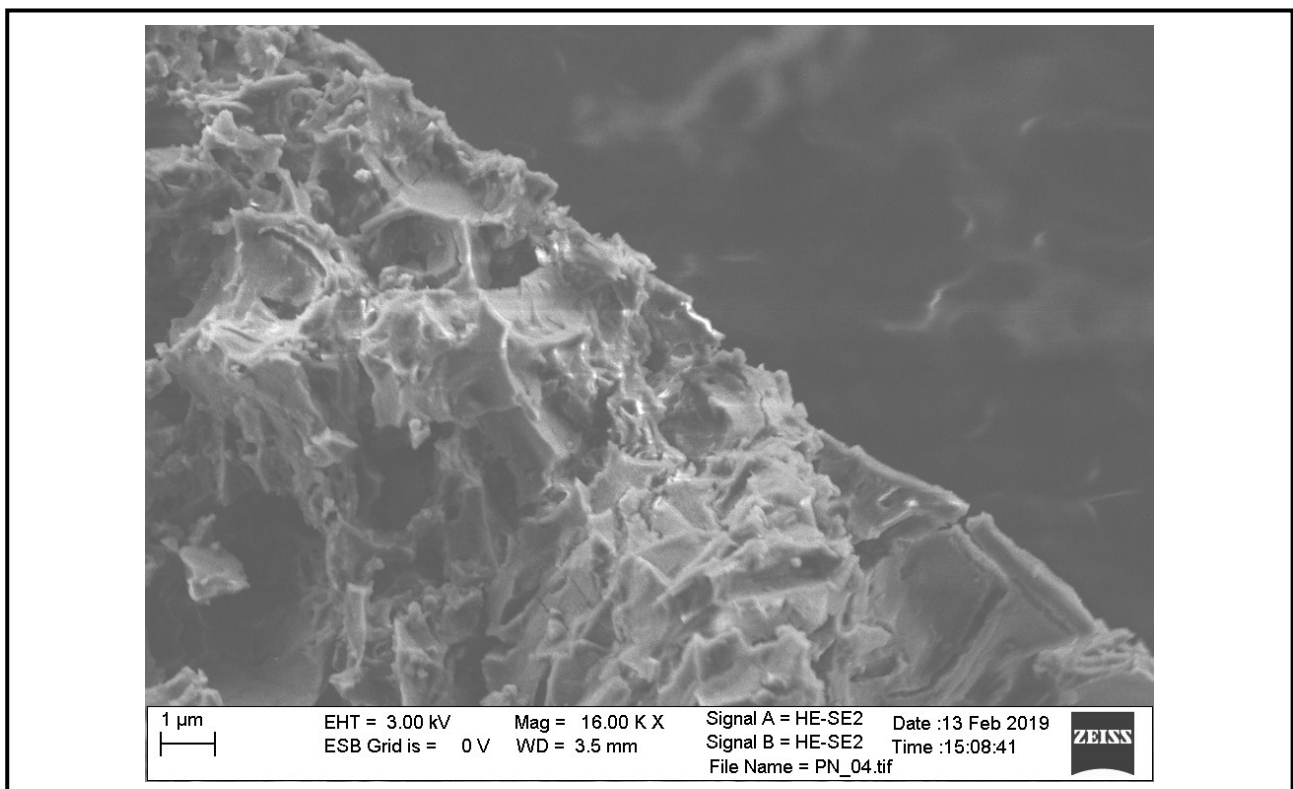


Figure S8.3. SEM image of $(\text{NH}_4)_3\text{Mg}(\text{BH}_4)_5$ sample heated to 650°C and rinsed 5 times with water. Magnification 16.00 KX

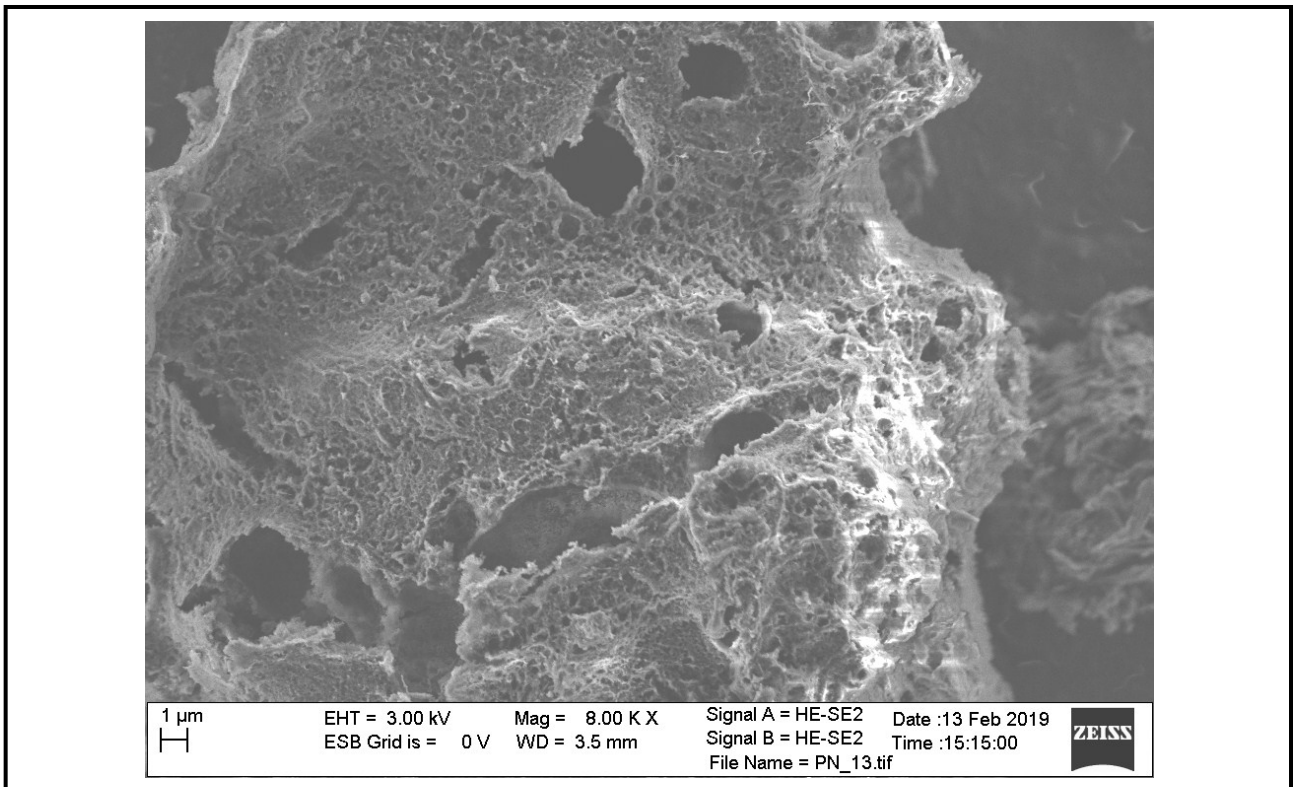


Figure S8.3. SEM image of $(\text{NH}_4)_3\text{Mg}(\text{BH}_4)_5$ sample heated to 650°C and rinsed 5 times with water. Magnification 8.00 KX

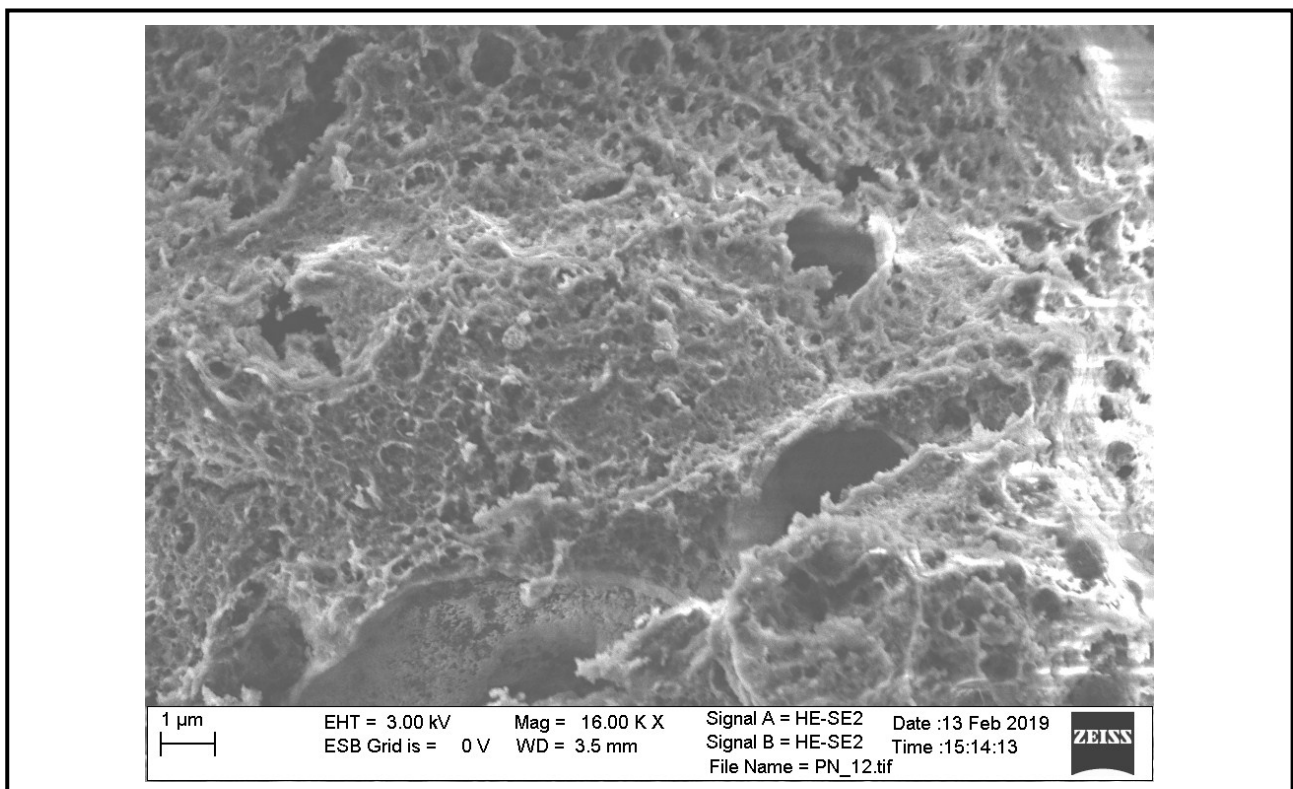


Figure S8.3. SEM image of $(\text{NH}_4)_3\text{Mg}(\text{BH}_4)_5$ sample heated to 650°C and rinsed 5 times with water. Magnification 16.00 KX

9. Calculation of the yield of pyrolytic BN synthesis: elemental analysis and gravimetric study

Elemental analysis. Thermally treated samples were tested for H, N contents analysis using 240 Perking Elmer analyser (detectability: 0.2 wt%, uncertainty: 0.3 wt%). Cl level was determined using potentiometric-argentometric method with AgNO₃ titration (detectability: 0.3 wt.%, uncertainty: 0.3 wt.%). Due to hygroscopic nature of by-products analyses for H contents are not reliable due to adsorbed water.

Elemental atomic concentration was normalised in respect to chlorine content which is stable in the sample throughout the pyrolysis, and equals 5 atoms per formula unit. Nitrogen content in the samples heated above 200°C is also constant and equals *c.a.* 2.2–2.3 atoms per formula unit, which is 75% of the initial nitrogen content in (NH₄)₃Mg(BH₄)₅·5LiCl.

Table S9.1. Elemental analysis of (NH₄)₃Mg(BH₄)₅ samples heated to 250°C, 500°C and 650°C, tested for hydrogen, nitrogen and chlorine. Concentration of said elements were normalised considering constant content of chlorine in the sample equal to 5 atoms per formula unit.

| [%] | 250°C [wt.%] | 250°C [norm. at.] | 500°C [wt.%] | 500°C [norm. at.] | 650°C [wt.%] | 650°C [norm. at.] |
|-----|-----------------|----------------------|-----------------|----------------------|-----------------|----------------------|
| H | 0.925 | 3.325 | 0.415 | 1.335 | 0.74 | 2.630 |
| N | 8.905 | 2.304 | 9.955 | 2.305 | 8.89 | 2.273 |
| Cl | 48.92 | 5 | 54.66 | 5 | 49.495 | 5 |

Gravimetric study. A 163 mg batch of (NH₄)₃Mg(BH₄)₅·5LiCl sample was heated to 650°C with heating rate of 5°C/min at inert atmosphere. Colourless powder was obtained and further subjected to washing procedure under air. The sample was rinsed 5 times with fresh portions of distilled water and yielded 30 mg product (Table S9.2).

The yield of pyrolytic synthesis of BN was calculated with respect to the model described in the Table S10, where the sample heated to 650°C (before rinsing) contains a mixture of BN, MgB₁₂H_x, MgH_y and 5 LiCl, where BN concentration equals 18.3 wt.%. 99% of the theoretic yield (i.e. 74 rather than 75%) of pyrolytic BN synthesis was achieved.

Table S9.2. Gravimetric study of (NH₄)₃Mg(BH₄)₅ pyrolysis towards BN at 650°C.

| Starting mass | Rinsed 3 times | Rinsed 5 times |
|-------------------|---------------------|---------------------|
| 163 mg (100 wt.%) | 32.3 mg (19.7 wt.%) | 30.0 mg (18.3 wt.%) |

10. Reaction route of pyrolytic BN synthesis

Already at RT, small fraction of NH_4BH_4 was detected in the samples of $(\text{NH}_4)_3\text{Mg}(\text{BH}_4)_5$ suggesting spontaneous decomposition of the complex, yet without evolution of neither hydrogen nor diborane and borazine.

The first step of thermal decomposition of $(\text{NH}_4)_3\text{Mg}(\text{BH}_4)_5$ occurs in the temperature range of 20–50°C and consists of a highly exothermic evolution of hydrogen and diborane resulting in *c.a.* 5.7 wt.% total mass loss. In this aspect, $(\text{NH}_4)_3\text{Mg}(\text{BH}_4)_5$ is similar to $\text{NH}_4\text{M}(\text{BH}_4)_4$ M = Y, Sc, Al and NH_4BH_4 , which decompose at relatively low temperatures below 60°C via a similar $(\text{H}^{\delta+})\cdots(\text{H}^{\delta-})$ coupling process.

When the sample of $(\text{NH}_4)_3\text{Mg}(\text{BH}_4)_5$ is kept at RT or at 60°C its PXRD pattern significantly changes (Figure 3 in the main manuscript). Time resolved PXRD patterns at room temperature show fading reflections of $(\text{NH}_4)_3\text{Mg}(\text{BH}_4)_5$ and NH_4BH_4 , as well as formation of NH_3BH_3 and an unknown phase (denoted *), which remains visible after thermal treatment at 60°C, while NH_3BH_3 vanishes. The pattern of the unknown phase (*) does not match the pattern of $\text{Mg}(\text{BH}_4)_2\cdot(\text{NH}_3\text{BH}_3)_2$ [2] nor of any known polymorph of $\text{Mg}(\text{BH}_4)_2$ [5]. However, it (*) resembles the pattern of $\text{MgB}_{12}\text{H}_{12}\cdot 3\text{H}_2\text{O}$ [3], which unit cell parameters are slightly different than those found for the phase (*) suggesting formation of $\text{MgB}_{12}\text{H}_{12}\cdot x\text{H}_2\text{O}$ when exposed to air for a very short time.

The analysis given below is based on the following hypothetical equality:



Purely for sake of quantifying elemental contents at various stages of thermal decomposition we oversimplify the description by silently assuming that Eq.S2 might actually correspond to a chemical reaction taking place at low or room temperature, i.e. before the first step of thermal decomposition as seen in TGA-DSC measurements. This assumption does not need to correspond to any true chemical reaction but it helps us to formalize calculations and separately describe phases containing and not containing Mg. It should be understood that with or without this simplification the net result would be identical but the description would be more difficult to follow by the reader.

NH_4BH_4 decomposes to NH_3BH_3 and $[\text{NH}_3\text{BH}_2\text{NH}_3]^+[\text{BH}_4]^-$ up to 50°C with the evolution of hydrogen molecule (Eq.S3a–Eq.S3b, mass loss 1.66 wt.% of the sample including LiCl dead mass) [4].



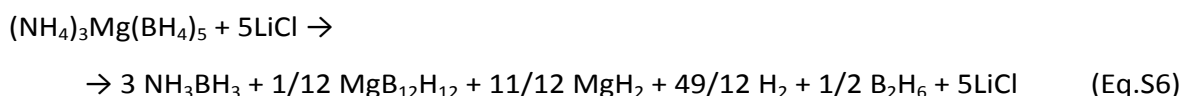
Since no diammoniate of diborane was observed in the investigated samples, the isomeric ammonia borane seems to be the sole product of NH_4BH_4 decomposition as discussed below.

Decomposition of $\text{Mg}(\text{BH}_4)_2$ may undergo two competing pathways, either to MgH_2 with evolution of B_2H_6 (Eq.4S, mass loss 7.59 wt.% of the sample) [5,6] or to mixture of $\text{MgB}_{12}\text{H}_{12}$ and MgH_2 with evolution of hydrogen (Eq.S5, mass loss 1.20%) [5,7].

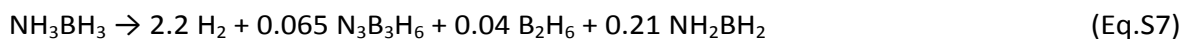


The 5.7 wt.% mass loss observed in TGA profile up to 50°C (Figure 2) is much lower than that predicted according to Eq.S3 and Eq.S4 (9.25 wt.%), and much higher than Eq.S3 and Eq.5 (2.86 wt.%).

This suggests that decomposition $(\text{NH}_4)_3\text{Mg}(\text{BH}_4)_5$ should be a combination of reactions Eq.S3–Eq.S5. Importantly, 100% completion of Eq.3 and 50% completion of Eq.S4–Eq.S5 (*i.e.* in ratio 1:1) would result in *c.a.* 6.0 wt.% mass loss, in fair agreement with TGA result and further PXRD and FTIR analyses. This scenario is shown in the following reaction equation (Eq.S6).



The second step of thermal decomposition of what was initially $(\text{NH}_4)_3\text{Mg}(\text{BH}_4)_5$ commences at *c.a.* 70°C. This process is composed of several distinct exothermic stages seen at DSC curve up to 250°C. An average total mass loss in the range of 20–650°C is equal to 16.8 wt.%. Above 70°C we have observed evolution of a mixture of hydrogen and borazine. Note that $\text{NH}_4\text{M}(\text{BH}_4)_4$ M = Y, Sc, Al decompose at the similar temperature range but without borazine evolution [8], while $\text{NH}_4\text{Ca}(\text{BH}_4)_3$ decomposes above 125°C, with a release of H_2 slightly contaminated with NH_3 , while yielding $\beta\text{-Ca}(\text{BH}_4)_2$. This suggests that traces of borazine originate from ammonia borane as well documented in the literature [9,10]:



Two distinct ranges of intensive hydrogen evolution were observed at 70–180°C and 200–250°C. According to time resolved QMS data, the amount of hydrogen released above 70°C was found to be *c.a.* 3.25 time larger than amount of H_2 evolved below 50°C. As already said, evolution of borazine was overlapping with evolution of hydrogen at 70–160°C resembling decomposition pattern of NH_3BH_3 (Eq.S7) [11]. No evolution of diborane was observed which suggest that all $\text{Mg}(\text{BH}_4)_2$ was consumed in reactions Eq.3 and Eq.4. Above 200°C evolution of pure hydrogen was observed which can be explained by decomposition of $\text{MgB}_{12}\text{H}_{12}$ (Eq.S8) [12] and MgH_2 (Eq.S9) [13].



The solid residues were rinsed with water to wash out all by-products. Yellow samples obtained at 220°C and 250°C almost entirely dissolved in water which suggested appreciable amount of impurities, while colourless samples obtained at 500°C and 650°C yielded substantial amount of colourless insoluble product corresponding to a-BN.

Samples of thermally treated $(\text{NH}_4)_3\text{Mg}(\text{BH}_4)_5$ (220°C, 250°C, 500°C, 650°C) were studied with a range of instrumental analyses at RT. All samples have similar PXRD patterns (Figure 3 in main paper) with predominating reflections of LiCl, along with MgO and a minor unknown phase (denoted #), which reflections clearly arise at higher temperatures. Most likely, MgO is formed when thermally treated sample exposed for a short period of time to aerobic atmosphere (it was impossible in our setup to manipulate the samples exclusively inside the glovebox) when expected MgH_2 reacts with oxygen [6]. Similarly, Ln_2O_3 were observed in thermally treated Ln– BH_4 systems [14]. Samples heated to 500°C and rinsed with water contained no crystalline products according to PXRD analysis (ESI), since LiCl, MgO and all unknown phases were washed out.

The FTIR spectra of the samples treated above 200°C contain bands characteristic to a-BN, around 1400 cm^{-1} and 800 cm^{-1} (Figure 4). Investigation of the solid residue with MAS NMR showed a doublet at *c.a.* +20 ppm at ^{11}B spectrum of the sample heated to 650°C (Figure 5). Comparative measurement of commercially available h-BN showed almost identical spectrum with all signals present in spectra

of both samples (Figure 5). Additionally, no signals were observed in the ^{15}N spectra collected for the same sample, which indicates absence of N–H bonds in the investigated material.

The SEM and EDX analyses (ESI, paragraph 8) of a sample treated at 650°C and rinsed with water indicated high purity of BN obtained. The average atomic ratio of boron to nitrogen was equal to 1:1.02, which is in good agreement with BN composition (ESI, part 8). Measurements show also *c.a.* 1 at% of Mg and 0.02 at% of Cl in the sample, confirming that almost all impurities were removed from the sample when rinsing with water.

Elemental analysis of the series of samples thermally treated above 200°C showed a nearly constant ratio of nitrogen to chloride equals to 2.25:5, proving that no emission of nitrogen-containing volatiles takes place after emission of borazine is completed. Considering that nitrogen to chloride ratio was 3:5 at the freshly prepared sample suggests that decomposition of NH_4BH_4 and further NH_3BH_3 undergoes in 25% the route towards borazine and in 75% a route towards BN.

Sequence of NH_3BH_3 decomposition reactions leading to BN are presented simplified in Eq.S10:



However full dehydrogenation of ammonia borane is known to occur at very high temperatures of $1170\text{--}1500^\circ\text{C}$ [11], specific conditions at chemical nature of $(\text{NH}_4)_3\text{Mg}(\text{BH}_4)_5$, with *in situ* forming NH_3BH_3 and $\text{Mg}(\text{BH}_4)_2$, seems to facilitate boron nitride formation at temperatures as low as 220°C in presence of various thermal decomposition mid-products. Full conversion to BN needs, however, further treatment at temperatures of $500\text{--}650^\circ\text{C}$ to accomplish dehydrogenation of the mid-products. Temperature of 650°C seems to be optimum since $\text{MgB}_{12}\text{H}_{12}$ decomposes to insoluble boron above 800°C which would make purification by water washing impossible.

Total yield of BN formation from $(\text{NH}_4)_3\text{Mg}(\text{BH}_4)_5$ was estimated to be 75% in respect of nitrogen content derived from elemental analysis, which was confirmed by gravimetric study (section 9 of this SI) showing 99% of this theoretical yield. $(\text{NH}_4)_3\text{Mg}(\text{BH}_4)_5$ decomposes to the mixture of NH_4BH_4 and $\text{Mg}(\text{BH}_4)_2$ which instantly undergo further decomposition to NH_3BH_3 , $\text{MgB}_{12}\text{H}_{12}$ and MgH_2 with evolution of hydrogen and diborane at temperature range $20\text{--}50^\circ\text{C}$. Further, the mid products decompose further: NH_3BH_3 partially release borazine and partially dehydrogenate towards BN, while $\text{MgB}_{12}\text{H}_{12}$ and MgH_2 loose most of hydrogen forming water soluble by-products.

Rietveld analysis of the pattern of $(\text{NH}_4)_3\text{Mg}(\text{BH}_4)_5$ heated to 650°C was done. The analysis gave mass ratio of LiCl to MgO equal to 7.85:1, which is in good agreement with the ratio 7.82:1 calculated according to the proposed reaction of total decomposition of $(\text{NH}_4)_3\text{Mg}(\text{BH}_4)_5$ suggesting formation of 11/12 molar equivalent of MgO and 1/12 equivalent of $\text{MgB}_{12}\text{H}_x$ in the product.

Summary of the proposed decomposition scenario is shown in the table below.

Table S10. Summary of theoretical partials reactions upon thermal decomposition of $(\text{NH}_4)_3\text{Mg}(\text{BH}_4)_5 \cdot 5\text{LiCl}$ at 650°C leading to amorphous boron nitride.

| | |
|----------------|--|
| SUBSTRATE: | $(\text{NH}_4)_3\text{Mg}(\text{BH}_4)_5 + 5 \text{LiCl}$ |
| factor | Partial reaction |
| 1 | $(\text{NH}_4)_3\text{Mg}(\text{BH}_4)_5 \rightarrow 3 \text{NH}_4\text{BH}_4 + \text{Mg}(\text{BH}_4)_2$ |
| 3 | $\text{NH}_4\text{BH}_4 \rightarrow \text{NH}_3\text{BH}_3 + \text{H}_2$ |
| 1/2 | $\text{Mg}(\text{BH}_4)_2 \rightarrow \text{MgH}_2 + \text{B}_2\text{H}_6$ |
| 1/2 | $\text{Mg}(\text{BH}_4)_2 \rightarrow 1/6 \text{MgB}_{12}\text{H}_{12} + 5/6 \text{MgH}_2 + 13/6 \text{H}_2$ |
| MID-PRODUCT: | $3 \text{NH}_3\text{BH}_3 + 1/12 \text{MgB}_{12}\text{H}_{12} + 11/12 \text{MgH}_2 + 49/12 \text{H}_2 + 1/2 \text{B}_2\text{H}_6 + 5\text{LiCl}$ |
| Factor | Partial reaction |
| 3/4 | $\text{NH}_3\text{BH}_3 \rightarrow 1/3 \text{N}_3\text{B}_3\text{H}_6 + 2\text{H}_2$ |
| 9/4 | $\text{NH}_3\text{BH}_3 \rightarrow \text{BN} + 3\text{H}_2$ |
| 1/12 | $\text{MgB}_{12}\text{H}_{12} \rightarrow \text{MgB}_{12}\text{H}_x + (12-x) \text{H}_2$ |
| 11/12 | $\text{MgH}_2 \rightarrow \text{MgH}_y + (1-y) \text{H}_2$ |
| FINAL PRODUCT: | $9/4 \text{BN} + 1/4 \text{N}_3\text{B}_3\text{H}_6 + 1/2 \text{B}_2\text{H}_6 + 1/12 \text{MgB}_{12}\text{H}_x + 11/12 \text{Mg} + 53/4 \text{H}_2 + 5 \text{LiCl}$ |

-
- [1] H. M. Colquhoun, G. Jones, J. M. Maud, J. F. Stoddart, D. J. Williams, *J. Chem. Soc. Dalt. Trans.*, 1984, 63.
- [2] X. Chen, F. Yuan, Q. Gu and X. Yu, *Dalt. Trans.*, 2013, **42**, 14365–14368.
- [3] X. Chen, Y.-H. Liu, A.-M. Alexander, J. C. Gallucci, S.-J. Hwang, H. K. Lingam, Z. Huang, C. Wang, H. Li, Q. Zhao, U. S. Ozkan, S. G. Shore and J.-C. Zhao, *Chem. - A Eur. J.*, 2014, **20**, 7325–7333.
- [4] A. Karkamkar, S. M. Kathmann, G. K. Schenter, D. J. Heldebrant, N. Hess, M. Gutowski and T. Autrey, *Chem. Mater.* 2009, **21**, 4356–4358
- [5] O. Zavorotynska, A. El-Kharbachi, S. Deledda, B.C. Hauback, *Int. J. Hydrog. Energy*, 2016, **41**, 14387.
- [6] S. Guo, H.Y.L. Chan, D. Reed, D. Book, *J. Alloy Compd.*, 2013, **580**, S296.
- [7] a) S. Gupta, I.Z. Hlova, T. Kobayashi, R.V. Denys, F. Chen, I.Y. Zavaliy, M. Pruski and V.K. Pecharsky, *Chem. Commun.* 2013, **49**, 828;
 b) H. W. Li, K. Kikuchi, Y. Nakamori, N. Ohba, K. Miwa, S. Towata and S. Orimo, *Acta Mater.*, 2008, **56**, 1342;
 c) Y. Yan Y, H.W. Li, Y. Nakamori, N. Ohba, K. Miwa, S. Towata, and S. Orimo, *Mater. Trans.* 2008, **49**, 2751;
 d) H. W. Li, K. Miwa, N. Ohba, T. Fujita, T. SatT, Y. Yan, S. Towata, M.W. Chen and S. Orimo, *Nanotech.*, 2009, **20**, 204013.
- [8] A. Starobrat, T. Jaroń and W. Grochala, *Dalt. Trans.*, 2018, **47**, 4442–4448.
- [9] G. Wolf, J. Baumann, F. Baitalow and F. P. Hoffmann, *Thermochimica Acta*, 2000, **343**, 19 .
- [10] F. Baitalow, J. Baumann, G. Wolf, K. Jaenicke-Röbler and G. Leitner, *Thermochimica Acta*, 2002, **391**, 159.
- [11] S. Frueh, R. Kellett, C. Mallery, T. Molter, W. S. Willis, C. King'onde, S. L. Suib, *Inorg. Chem.*, 2011, **50**, 783.
- [12] L. He, H. W. Li, N. Tumanov, Y. Filinchuk, E. Akiba, *Dalton Trans.*, 2015, **44**, 15882.
- [13] W. Grochala and P. P. Edwards, *Chem. Rev.*, 2004, **104**, 1283–1315.
- [14] W. Wegner, T. Jaroń, W. Grochala, *Journal of Alloys and Compounds*, 2018, **744**, 57.